

# Equatorial undercurrents associated with Indian Ocean Dipole events during contrasting summer monsoons

P. Swapna<sup>1,2</sup> and R. Krishnan<sup>1</sup>

Received 27 January 2008; revised 10 March 2008; accepted 18 March 2008; published 23 April 2008.

[1] Positive Indian Ocean Dipole (IOD) events generally tend to be accompanied by intensified summer monsoon flows and above normal precipitation over the sub-continent; although strong monsoons have not always coincided with positive IOD events. Numerical simulation experiments and supplementary data diagnostics are performed to understand the IOD sub-surface dynamics in relation to the monsoon strength. The model experiments when forced by IOD winds during strong monsoon periods generated a strong subsurface zonal pressure gradient along the equator and an eastward equatorial undercurrent (EUC) leading to supply of cold subsurface waters to the upwelling regions in the eastern equatorial Indian Ocean. However, the simulations when forced with IOD winds during weak monsoon periods were unable to set up the subsurface pressure gradients and the EUC, thus resulting in weak SST cooling in the east. These results raise the possibility that IOD-monsoon interactions during strong monsoon years might favor intensification of the IOD. **Citation:** Swapna, P., and R. Krishnan (2008), Equatorial undercurrents associated with Indian Ocean Dipole events during contrasting summer monsoons, *Geophys. Res. Lett.*, 35, L14S04, doi:10.1029/2008GL033430.

## 1. Introduction

[2] Advances in our understanding of ocean-atmosphere interactions in the tropical Indian Ocean (IO) together with insights gained from the IOD phenomenon have established the importance of IO dynamics on the regional climate variability [e.g., *Saji et al.*, 1999; *Webster et al.*, 1999; *Behera et al.*, 1999; *Murtugudde et al.*, 2000]. Positive IOD events often tend to be accompanied by enhanced summer monsoon precipitation over the Indian subcontinent [*Behera et al.*, 1999; *Ashok et al.*, 2004], due to increased supply of moisture from the southeastern tropical Indian Ocean (SETIO). Thus, while IOD years can induce precipitation enhancement over India, it is not clear whether the intensified monsoonal wind anomalies can influence the ocean dynamics. Understanding this problem is important because the issue of IOD-monsoon interaction has implications on regional climate variability [*Yamagata et al.*, 2004, *Annamalai and Murtugudde*, 2004].

[3] The studies by *Vinayachandran et al.* [1999] and *Murtugudde et al.* [2000] discussed the role of ocean

dynamics on IOD evolution and pointed out the importance of eastward equatorial undercurrents (EUC) in the IO. Unlike the Pacific and Atlantic Oceans, consistent EUC is observed during boreal spring in the IO and is highly transient in nature [Schott and McCreary, 2001]. Current-meter observations by *Reppin et al.* [1999] showed the presence of EUC in the IO during the summer of 1994 – a well-known IOD associated with heavy monsoon rainfall over India [*Behera et al.*, 1999]. The presence of EUC in the IO is also reported during the 2006 IOD [Lakshmi et al., 2007]. Given that IOD events peak during the autumn months following the boreal summer monsoon, it is not clear whether the intensification of the monsoon flow can actually feedback on the ocean dynamics. In other words, it is not obvious as to whether the strength of the monsoon circulation can affect the IOD response. In this study, we examine the EUC and sub-surface pressure gradients of IOD events between strong and weak monsoons. Section 2 describes the datasets and ocean model. Section 3 presents analyses of the model simulations and section 4 discusses the results.

## 2. Datasets, Ocean Model and Experiments

[4] The data diagnostics include surface winds from National Center for Environmental Prediction (NCEP) reanalysis [Kistler et al., 2001], SST from the HadISST1.1 dataset [Rayner et al., 2003], CPC Merged Analysis of Precipitation (CMAP) dataset [Xie and Arkin, 1997] and Simple Ocean Data Assimilation (SODA) [Carton et al., 2000]. Except the CMAP rainfall which is available since 1979, other datasets are for the period (1958–2006). The ocean general circulation model used in this study is based on the model developed at Institute of Numerical Mathematics (INM), Russia [Alekseev and Zalesny, 1993]. The governing equations are the primitive equations of motion in spherical sigma co-ordinates, with hydrostatic, Boussinesq and rigid-lid approximations.

[5] The model domain covers the tropical IO (22°E to 142°E; 36°S to 29.5°N) and has a moderate resolution of (1° × 0.5°) with 33 sigma levels in the vertical. *Saji et al.* [2006] compared the INM model with other Intergovernmental Panel on Climate Change (IPCC) models and found better performance of INM for IOD events. The model was initialized with the temperature and salinity fields from World Ocean Atlas (WOA2001, <http://www.nodc.noaa.gov/OC5/WOD01>) and was integrated for 10 years. The climatological forcing derived from NCEP reanalysis were provided during the spin-up period. Temperature and salinity values from WOA2001 are specified at the open boundaries at 36°S and 142°E. Following the spin-up, the

<sup>1</sup>Indian Institute of Tropical Meteorology, Pune, India.

<sup>2</sup>Now at Atmospheric, Marine and Coastal Environment Program, Hong Kong University of Science and Technology, Hong Kong.

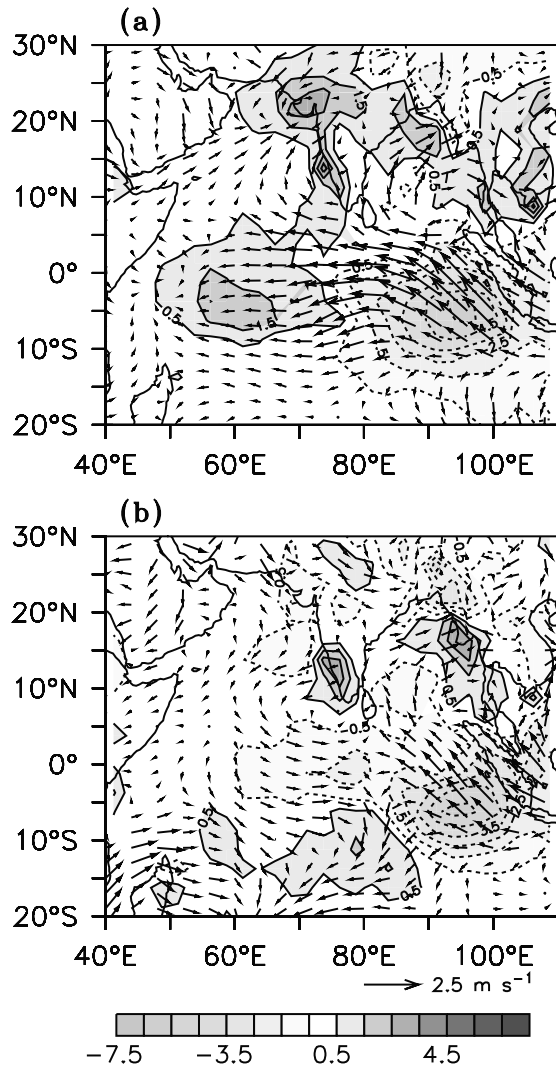


**Figure 1.** Anomaly composites of surface winds ( $\text{ms}^{-1}$ ) and rainfall ( $\text{mm day}^{-1}$ ) for June to September (JJAS) monsoon season (a) Strong monsoon IOD years (b) Weak monsoon IOD years. The wind anomalies for the STRMON composite are based on 8 cases (1961, 1963, 1967, 1977, 1983, 1994, 1997, 2006) and for the WKMON composite are based on 3 cases (1972, 1982, 1991). Since the CMAP rainfall data is available from 1979 onward, we have used 4 STRMON cases and 2 WKMON cases for rainfall composite.

interannual simulations of the model were carried out for the period 1960–2006.

### 3. The IOD Events During Contrasting Monsoon Years

[6] Using the different datasets, we first compare the IOD events during the strong and weak monsoon years. According to the India Meteorological Department, excess (deficit) monsoons are defined when the all-India rainfall during June–September months is more (less) than 10% of the long-term climatological normal  $\sim 853$  mm. The time-series of the all-India monsoon rainfall anomalies for the period

(1958–2006) is shown in Figure S1<sup>1</sup> along with the positive IOD events. There were eleven positive IOD events in the past 50 years - during 1961, 1963, 1967, 1972, 1977, 1982, 1983, 1991, 1994, 1997 and 2006. While Meyers *et al.* [2007] classify 1991 as a positive-IOD, some studies consider it as an El Niño event rather than a positive IOD [e.g., Yamagata *et al.*, 2003, 2004]. However, we have included 1991 in our analysis because it was case of a weak monsoon and such instances (weak monsoon + positive IOD) are relatively few. The precipitation was excess during 1961, 1983 and 1994 and above-normal during 1963, 1967, 1977, 1997 and 2006. Precipitation was deficit during 1972 and 1982 and below-normal in 1991.

[7] Anomaly composites of rainfall and surface winds are shown in Figure 1 for the stronger-than-normal monsoons (STRMON). The NCEP wind anomalies are based on the years (1961, 1963, 1967, 1977, 1983, 1994, 1997 and 2006) and the rainfall anomalies for (1983, 1994, 1997 and 2006) since the CMAP data is from 1979 onward. The wind anomalies show strong easterlies extending across the IO basin between  $10^{\circ}\text{S}$ – $5^{\circ}\text{N}$  with strong southeasterly anomalies off Sumatra-Java. Since the boreal summer climatological winds are southeasterly to the south of the equator, the wind anomalies basically indicate an intensification of the mean-flow. Strong southwesterly anomalies are seen to the north of  $10^{\circ}\text{N}$  over the Bay of Bengal and Arabian Sea. The rainfall anomalies for June–September months show enhancement of precipitation over the western equatorial IO and the Indian landmass along the west coast and Bay of Bengal. A zone of anomalous convergence of winds is seen over the western equatorial IO around  $65^{\circ}\text{E}$ . In contrast, the weak monsoon (1972, 1982 and 1991) composite (WKMON) shows weak easterly anomalies over the equatorial IO and weak south-easterlies to the south of equator. The anomalous easterlies around  $10^{\circ}\text{N}$  over the Arabian Sea (Figure 1b) indicate a weakened summer monsoon flow. The monsoon rainfall anomalies over India and the dipole pattern of precipitation anomalies over the equatorial IO are weaker in Figure 1b as compared to Figure 1a.

#### 3.1. Ocean Response

[8] Current meter observations by Reppin *et al.* [1999] provided vital evidence for eastward Equatorial Undercurrents (EUC) in the equatorial IO during the summer of 1994. In the Pacific and Atlantic Oceans, the EUC is a quasi-permanent eastward current at the top of the thermocline, driven by the eastward pressure gradient force [Schott and McCreary, 2001]. In the IO, the EUCs are transient in nature. The current-meter observations by Masumoto *et al.* [2005] revealed eastward EUC between June–September of 2002, while the EUC was absent during summer of 1993 [Reppin *et al.*, 1999]. Earlier observations showed the EUC slightly to the south of equator [Leetmaa and Stommel, 1980]; although it was observed at  $2^{\circ}\text{N}$  during 1994.

[9] Longitude-depth sections of zonal current anomalies from SODA are shown for the STRMON and WKMON composites in Figures 2a and 2b, respectively. The anomalies are averaged between  $2^{\circ}\text{S}$ – $2^{\circ}\text{N}$  and shown for the

<sup>1</sup>Auxiliary materials are available in the HTML. doi:10.1029/2008GL033430.

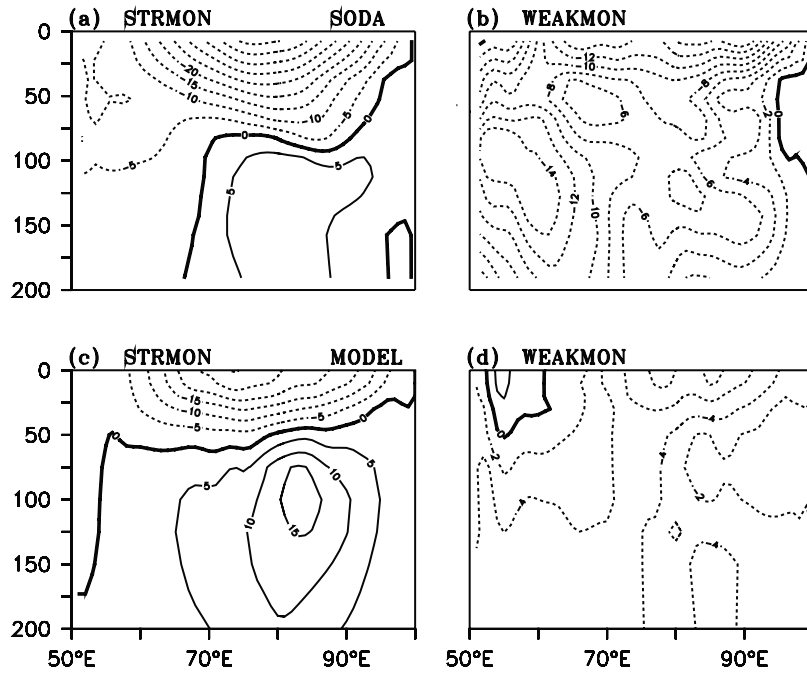


**Figure 2.** Longitude-depths sections show composite maps of zonal velocity anomalies ( $\text{cm s}^{-1}$ ) for JJAS from SODA (a and b) and OGCM (c and d). The solid (dashed) line represents eastward (westward) flow. Left (right) column shows strong-monsoon IOD (weak monsoon IOD) composites.

June–September (JJAS) season. In the STRMON composite (Figure 2a), anomalous westward currents are seen from surface to 100 m depth and anomalous eastward undercurrents near the 100 m depth and below. The westward anomalies are known to be forced by easterly wind anomalies [Murtugudde *et al.*, 2000; Feng *et al.*, 2001; Rao *et al.*, 2002]. The maximum eastward EUC anomaly is located between the 100–150 m depth with an eastward slope. The meridional structure of zonal velocity shows that the EUC anomalies extend slightly north of equator in the STRMON composite (Figure S2). The zonal current anomalies in the WKMON composite (Figure 2b) show westward anomalies extending from surface to about 200 m depth. It is also interesting that the eastward EUCs are not seen in the WKMON composite.

[10] The OGCM simulated zonal current anomalies for the STRMON and WKMON composites are shown in Figures 2c and 2d, respectively. The STRMON composite

exhibits westward anomalies in the near-surface layers with a maximum speed of  $30 \text{ cm sec}^{-1}$  and eastward EUC anomalies below 100 m depth with an eastward slope. In the WKMON composite, the simulation shows westward anomalies extending from the surface to 200 m depth (Figure 2b). We have further confirmed the relation between the strength of the summer time undercurrents and the strength of the IOD in the autumn months. Longitude-depth sections of zonal current and temperature anomalies are shown both for the summer (JJA) and autumn (SON) seasons in Figure S3. It can be seen that the peak season IOD anomalies in the STRMON composite exhibit intensified EUC anomalies and enhanced zonal temperature gradients as compared to the WKMON composite.

### 3.2. Mechanism of EUC

[11] The eastward EUCs are primarily driven by east–west pressure gradients in the equatorial region. Figure 3a

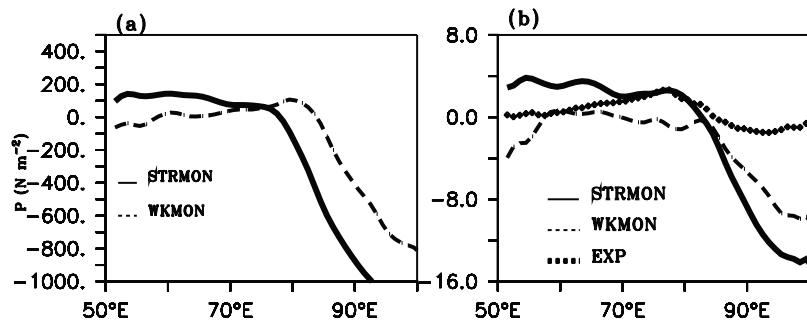


**Figure 3.** (a) Longitudinal variation of the model simulated pressure anomaly ( $\text{N m}^{-2}$ ) averaged between  $2^{\circ}\text{S}$ – $2^{\circ}\text{N}$  at 100 m depth for the JJAS season. The solid (dashed) line represents strong monsoon (weak monsoon) IOD years. (b) Same as Figure 3a, except for the  $20^{\circ}\text{C}$  isotherm depth ( $D_{20}$ , m). The line with symbol represents the  $D_{20}$  (m) for Oct–Nov from the sensitivity experiment. The positive (negative) values represent deepening (shoaling) of thermocline.

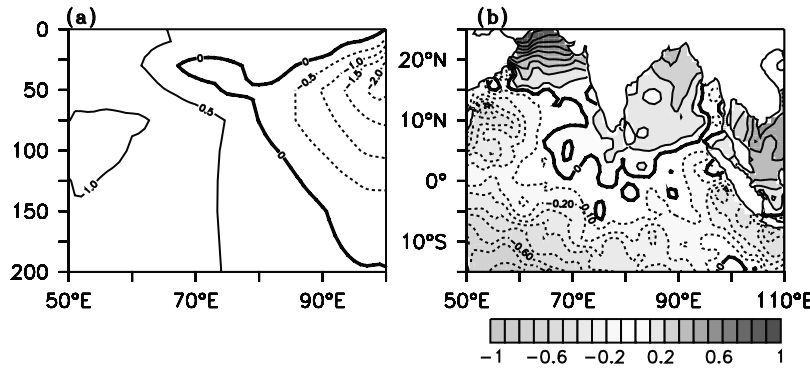


**Figure 4.** (a) Composite maps of subsurface temperature anomaly ( $^{\circ}\text{C}$ ) difference between the strong monsoon IOD and weak monsoon IOD composite years, averaged between  $10^{\circ}\text{S}$  and equator for JJAS from the model. (b) Sea surface temperature anomaly ( $^{\circ}\text{C}$ ) difference between STRMON and WKMON composite years.

shows the zonal variation of pressure anomaly from the model at 100 m depth, along the equator. It can be seen that the pressure anomaly in STRMON shows a significant pressure drop in the east. A maximum pressure drop of about  $1000 \text{ N m}^{-2}$  can be seen around  $95^{\circ}\text{E}$  and an anomalous pressure rise of about  $200 \text{ N m}^{-2}$  near  $65^{\circ}\text{E}$  on the western side. In the WKMON case, the pressure drop in the east is about  $800 \text{ N m}^{-2}$  and there is no significant pressure rise on the western side. Basically, the subsurface pressure gradient is weak in WKMON and hence cannot effectively drive the EUC. On the other hand, the STRMON case is characterized by a strong zonal pressure gradient along the equator which effectively drives the EUC. The east–west slope of the zonal pressure gradient is also consistently reflected in the east–west slope of the  $20^{\circ}\text{C}$  isotherm depth (D20) which is a proxy for the thermocline depth (Figure 3b). In the STRMON case (solid line), the thermocline is significantly deeper in the western IO and it shoals in the east. However, the east–west gradient of D20 is much weaker in the WKMON composite (dashed line).

[12] Though intensified summer monsoon winds tend to enhance the equatorial easterlies during IOD events, not all strong monsoon years were accompanied by IOD events. We performed a sensitivity experiment to understand this problem. The OGCM is forced with wind stress composites from strong monsoons that were not associated with IOD (i.e., 1956, 1959, 1970, 1975 and 1988). This wind-forcing is applied from January till September and then the winds are set to climatology. The D20 response from this experiment (Figure 3b) shows weak east–west gradient of D20 anomalies. This suggests that persistent easterly wind-forcing over the equator is essential for the generation of the subsurface zonal pressure gradient and the EUC. Such a strong easterly wind-forcing is provided by the combination of an IOD and an intensified summer monsoon circulation.

[13] The difference in the temperature response of IOD events between strong and weak monsoons can be inferred from Figure 4. The longitude-depth section of the difference (STRMON minus WKMON) in the temperature anomalies simulated by the model is shown in Figure 4a. The subsurface cooling in the east is enhanced by nearly  $2^{\circ}\text{C}$  during STRMON as compared to WKMON. The sea surface

temperature anomaly (SSTA) difference between the STRMON and WKMON composites is shown in Figure 4b. Notice that the SST cooling in the SETIO is enhanced in STRMON by more than  $-0.5^{\circ}\text{C}$  as compared to WKMON.

#### 4. Discussion

[14] Several strong positive IOD events in the past were accompanied by above-normal precipitation over the Indian landmass. Since the IOD phenomenon evolves through the boreal summer and attains peak amplitude during autumn, we examined the potential role of the monsoon flow in shaping the IO dynamics during IOD events. This study is based on model simulation experiments and analyses of data products from multiple-sources. The results suggest that IOD events during strong monsoons tend to be characterized by strong eastward EUC anomalies at sub-surface depths near 100 m, along with westward anomalies in the near-surface layers. The intensified EUC anomalies were found to be driven by equatorial zonal pressure gradients arising from a pressure drop in the east and a pressure rise in the west. The enhanced EUCs associated with strong-monsoon IOD events deliver cold subsurface waters to the upwelling regions in the eastern IO and thereby maintain the strong cooling in the region. On the other hand, the IODs during weak monsoon years did not reveal the eastward EUC anomalies. In the latter case, the equatorial zonal pressure gradient in the sub-surface was found to be much weaker. It was noted that the SST cooling in the SETIO for IOD events is enhanced during strong monsoon years by more than  $-0.5^{\circ}\text{C}$  as compared to IODs during weak-monsoons. Based on the findings, it is suggested that the intensity of the summer monsoon circulation is an important element that can determine the zonal contrast of the ocean temperature anomalies during IOD events. Further studies using coupled models will be required to unravel the details of the ocean-atmosphere feedbacks associated with IOD-monsoon interactions.

[15] **Acknowledgments.** The authors thank the Director, IITM, for the encouragement and support to carry out this research. The model was provided by N. A. Diansky, INM, Russia. The authors thank the Editor Anne Muller and the two anonymous reviewers for their helpful comments

and suggestions. This work was supported under the DOD/INDOMOD-SATCORE (ISP 1.5) project, Govt. of India.

## References

- Alekseev, V. V., and V. B. Zalesny (1993), Numerical model of large scale dynamics of ocean (in Russian), in *Computing Processes and Systems*, vol. 10, edited by G. I. Marchuk, pp. 232–252, Nauka, Moscow.
- Annamalai, H., and R. Murtugudde (2004), Role of the Indian Ocean in regional climate variability, in *Earth's Climate: The Ocean-Atmosphere Interaction, Geophys. Monogr. Ser.*, vol. 147, edited by C. Wang, S.-P. Xie, and J. A. Carton, pp. 213–246, AGU, Washington, D. C.
- Ashok, K., Z. Guan, N. H. Saji, and T. Yamagata (2004), On the individual and combined influence of the ENSO and the Indian Ocean dipole on the Indian summer monsoon, *J. Clim.*, 17, 3141–3154.
- Behera, S. K., R. Krishnan, and T. Yamagata (1999), Unusual ocean-atmosphere conditions in the tropical Indian Ocean during 1994, *Geophys. Res. Lett.*, 26, 3001–3004.
- Carton, J. A., G. Chepurin, X. Cao, and B. Giese (2000), A simple ocean data assimilation analysis of the upper ocean 1950–95. part I: Methodology, *J. Phys. Oceanogr.*, 30, 294–309.
- Feng, M., G. Meyers, and S. Wijffels (2001), Interannual upper ocean variability in the tropical Indian Ocean, *Geophys. Res. Lett.*, 28, 4151–4154.
- Kistler, R., et al. (2001), The NCEP/NCAR 50-year reanalysis: Monthly means CDROM and documentation, *Bull. Am. Meteorol. Soc.*, 82, 247–268.
- Lakshmi, A. S. N., et al. (2007), Semi-annual variability in the observed and OGCM simulated zonal currents in the equatorial Indian Ocean, paper presented at Celebrating the Monsoon: An International Monsoon Conference, Indian Inst. of Sci., Bangalore, India, 24–28 Jul.
- Leetmaa, A., and H. Stommel (1980), Equatorial current observations in the western Indian Ocean in 1975 and 1976, *J. Phys. Oceanogr.*, 10, 258–269.
- Masumoto, Y., H. Hase, Y. Kuroda, H. Matsuura, and K. Takeuchi (2005), Intraseasonal variability in the upper layer currents observed in the eastern equatorial Indian Ocean, *Geophys. Res. Lett.*, 32, L02607, doi:10.1029/2004GL021896.
- Meyers, G., P. McIntosh, L. Pigot, and M. Pook (2007), The years of El Niño, La Niña, and interactions with the tropical Indian Ocean, *J. Clim.*, 20, 2872–2880.
- Murtugudde, R. G., J. P. McCreary, and A. J. Busalacchi (2000), Oceanic processes associated with anomalous events in the Indian Ocean with relevance to 1997–1998, *J. Geophys. Res.*, 105, 3295–3306.
- Rao, S. A., S. K. Behera, Y. Masumoto, and T. Yamagata (2002), Interannual variability in the subsurface tropical Indian Ocean with a special emphasis on the Indian Ocean dipole, *Deep Sea Res., Part II*, 49, 1549–1572.
- Rayner, N. A., D. E. Parker, E. B. Horton, C. K. Folland, L. V. Alexander, D. P. Rowell, E. C. Kent, and A. Kaplan (2003), Global analyses of sea surface temperature, sea ice, and night marine air temperature since the late nineteenth century, *J. Geophys. Res.*, 108(D14), 4407, doi:10.1029/2002JD002670.
- Reppin, J., F. A. Schott, J. Fischer, and D. Quadfasel (1999), Equatorial currents and transports in the upper central Indian Ocean: Annual cycle and interannual variability, *J. Geophys. Res.*, 104, 15,495–15,514.
- Saji, N. H., B. N. Goswami, P. N. Vinayachandran, and T. Yamagata (1999), A dipole mode in the tropical Indian Ocean, *Nature*, 401, 360–363.
- Saji, N. H., S. P. Xie, and T. Yamagata (2006), Tropical Indian Ocean variability in the IPCC twentieth-century climate simulations, *J. Clim.*, 19, 4397–4417.
- Schott, F., and J. P. McCreary (2001), The monsoon circulation of the Indian Ocean, *Prog. Oceanogr.*, 51, 1–123.
- Vinayachandran, P. N., N. H. Saji, and T. Yamagata (1999), Response of the equatorial Indian Ocean to an anomalous wind event during 1994, *Geophys. Res. Lett.*, 26, 1613–1616.
- Webster, P. J., A. M. Moore, J. P. Loschnigg, and R. R. Leben (1999), Coupled ocean-atmosphere dynamics in the Indian Ocean during 1997–98, *Nature*, 401, 356–359.
- Xie, P., and P. Arkin (1997), A 17-year monthly climatology based on gauge observations, satellite estimates and numerical model outputs, *Bull. Am. Meteorol. Soc.*, 78, 2539–2558.
- Yamagata, T., S. K. Behera, S. A. Rao, Z. Guan, K. Ashok, and N. H. Saji (2003), Comments on “Dipoles, temperature gradients and tropical climate anomalies”, *Bull. Am. Meteorol. Soc.*, 84, 1418–1422.
- Yamagata, T., S. K. Behera, J. J. Luo, S. Masson, M. R. Jury, and S. A. Rao (2004), Coupled ocean-atmosphere variability in the tropical Indian Ocean, in *Earth's Climate: The Ocean-Atmosphere Interaction, Geophys. Monogr. Ser.*, vol. 147, edited by C. Wang, S.-P. Xie, and J. A. Carton, pp. 189–211, AGU, Washington, D. C.

R. Krishnan, Indian Institute of Tropical Meteorology, Pashan, NCL-Post, Pune, Maharashtra 411 008, India.

P. Swapna, AMCE, Hong Kong University of Science and Technology, Clear Water Bay, Kowloon, Hong Kong 852, Hong Kong. (panickal@ust.hk)